Received: 27 February 2020 | Revised: 10 October 2020 | Accepted: 12 October 2020

DOI: 10.1002/nla.2346

RESEARCH ARTICLE

WILEY

A novel direct method based on the Lucas multiwavelet functions for variable-order fractional reaction-diffusion and subdiffusion equations

Haniye Dehestani[1] | **Yadollah Ordokhani**[1] | **Mohsen Razzaghi**[2]

[1]Department of Mathematics, Faculty of Mathematical Sciences, Alzahra University, Tehran, Iran

[2]Department of Mathematics and Statistics, Mississippi State University, Starkville, Mississippi

Correspondence
Yadollah Ordokhani, Department of Mathematics, Faculty of Mathematical Sciences, Alzahra University, Tehran, Iran.
Email: ordokhani@alzahra.ac.ir

Abstract

In this article, we study the numerical technique for variable-order fractional reaction-diffusion and subdiffusion equations that the fractional derivative is described in Caputo's sense. The discrete scheme is developed based on Lucas multiwavelet functions and also modified and pseudo-operational matrices. Under suitable properties of these matrices, we present the computational algorithm with high accuracy for solving the proposed problems. Modified and pseudo-operational matrices are employed to achieve the nonlinear algebraic equation corresponding to the proposed problems. In addition, the convergence of the approximate solution to the exact solution is proven by providing an upper bound of error estimate. Numerical experiments for both classes of problems are presented to confirm our theoretical analysis.

KEYWORDS

Lucas multiwavelet functions, operational matrix, variable-order Caputo fractional derivative, variable-order fractional diffusion equation, variable-order fractional subdiffusion equation

1 | INTRODUCTION

During this decade, fractional calculus has gained considerable popularity in many branches of science and engineering but several experimental results disclosed that problems with fractional-order are not able to demonstrate the behavior of complex processes.[1] Several researchers have examined the problems by variable-order (VO) calculus, which understood that these problems are more accurate than problems by the constant-order to describe complex physical models.[2] These types of fractional derivatives create an extra degree of freedom for solving the VO fractional derivative problems. In addition, the nonlocal properties of VO fractional operators improve the computational accuracy and decrease the computational cost.

Recently, attention to the VO-fractional calculus in the modeling of phenomena in many branches of science and engineering has grown. Such as dynamics of the van der Pol equation, statistical mechanics model, and design of new control algorithms.[3-6] For more relevant references, the readers can refer to References 1,7.

Then, many numerical and analytical schemes have emerged to solve VO fractional problems, including the spline finite difference scheme,[8] the nonstandard finite difference method,[9] discrete schemes based on Genocchi-fractional Laguerre functions,[10] the pseudo-operational matrix (POM) method,[11] and the shifted the Legendre–Gauss–Lobatto collocation method.[12]

The object of this article is to develop the wavelet method together with Lucas polynomials for the numerical solution of VO-fractional diffusion and subdiffusion equations. The fractional diffusion and subdiffusion equations have been widely applied to the model of some phenomena or processes in various branches of science and engineering, see References 13-19 and references therein. In addition, many research articles have been published in this field that includes numerical methods. For instance, finite difference method,[20,21] the Monte Carlo Markov chain method,[22] wavelets Galerkin method,[23] and the cubic trigonometric B-spline collocation approach.[24]

The purpose of this article is to present a numerical method based on the Lucas multiwavelet functions (LMWFs), these functions are constructed from Lucas polynomials.[25,26] In addition, the proposed method includes the novel techniques for obtaining the modified operational matrix (MOM) of integration and POM of the VO-fractional derivative. In calculating the POM, the component that increases the error is included as a coefficient and exits to the approximation process. And also, in the calculation of the MOM, no component has been omitted. These methods offer high accuracy matrices compared with other available methods. The precision of these matrices reflect into the whole of the scheme and provide the approximate solutions with high accuracy. These polynomials have been applied for solving a variety of problems, for instance, Oruc[26,27] investigated the approximate solution of nonlinear generalized Benjamin–Bona–Mahony–Burgers equation and Sinh–Gordon equation.

Here, it is necessary to mention that wavelet methods have been getting more attention lately for solving different problems. For example, the Genocchi wavelet method for different kinds of fractional-order differential equations with delay,[28] the Legendre wavelets method for the numerical solutions of nonlinear Volterra integro-differential equations system,[29] Chebyshev cardinal wavelets for solving nonlinear stochastic differential equations with fractional Brownian motion,[30] and Chebyshev wavelet for solving the fractional Logistic differential equations.[31]

It must be pointed out that there are various numerical methods in the numerical analysis for the proposed equations. For the fractional diffusion equation, Zhang et al.[32] used the time-discrete scheme based on the finite difference method, Hajipour et al.[33] applied the Chebyshev wavelet approach for solving multiterm VO time-fractional diffusion-wave equation, Cao et al.[34] provided the compact finite difference operator for solving VO-fractional reaction–diffusion equation. For fractional subdiffusion equations, Yu et al.[35] applied the compact finite difference scheme for VO-fractional subdiffusion equations, Yaseen et al.[24] proposed the generalized Laguerre spectral Petrov–Galerkin method, Ghaffari and Ghoreishi[36] proposed a cubic trigonometric B-spline collocation approach, and so forth (see References 22,37-39).

1.1 | Outlines of the present article

The proposed method has many useful properties, but the most important one is the calculation of high-precision operational matrices that are effective in the overall method accuracy.

The organization of the present article is as follows: Section 2 introduces Lucas wavelet functions (LWFs) and their properties and also describes the transformation matrix of Lucas wavelets to the Taylor scaling functions (TSFs). In Section 3, we provide the method for obtaining the operational matrices. In Section 4, the method implementation for the VO-fractional diffusion equation and VO-fractional subdiffusion equation are presented in detail. Section 5 is devoted to error analysis of approximate solutions. In Section 6, numerical experiments are presented to illustrate the validity and applicability of the proposed method. Finally, in Section 7 concluding remarks are given.

1.2 | Notations and the problems statement

We consider two classes of VO-fractional problems by the following forms:

Problem 1: VO-fractional diffusion equation:[33]

$$\mathcal{D}_{0,t}^{\nu(t)}\mathfrak{U}(x,t) = \kappa\frac{\partial^2\mathfrak{U}(x,t)}{\partial x^2} + \mathcal{F}(x,t,\mathfrak{U}), \qquad (x,t)\in(0,1)\times(0,1], \tag{1}$$

with initial and boundary conditions

$$\begin{aligned}&\mathfrak{U}(x,0) = \varphi(x), \qquad x\in[0,1],\\ &\mathfrak{U}(0,t) = \omega_0(t), \qquad \mathfrak{U}(1,t) = \omega_1(t), \qquad t\in[0,1].\end{aligned}$$

Here, κ is the diffusion constant and $\mathcal{D}_{0,t}^{\nu(t)}$ is the VO Caputo fractional derivative of order $0 < \nu(t) \leq 1$ that is defined as follows:

$$\mathcal{D}_{0,t}^{\nu(t)}\mathfrak{U}(x,t) = \frac{1}{\Gamma(1-\nu(t))}\int_0^t \frac{\partial \mathfrak{U}(x,\eta)}{\partial \eta}(t-\eta)^{-\nu(t)}d\eta,$$

where $\Gamma(.)$ is the Gamma function and the fractional order $\nu(t)$ is a continuous function.

Problem 2: VO-fractional subdiffusion equation:[34]

$$\frac{\partial \mathfrak{U}(x,t)}{\partial t} = \mathcal{D}_{0,t}^{1-\nu(x,t)}\left[\kappa_1 \frac{\partial^2 \mathfrak{U}(x,t)}{\partial x^2} - \kappa_2 \mathfrak{U}(x,t)\right] + \mathcal{G}(x,t,\mathfrak{U}), \qquad (x,t) \in (0,1)\times(0,1], \tag{2}$$

with initial and boundary conditions

$$\begin{aligned} &\mathfrak{U}(x,0) = \varphi(x), \qquad x \in [0,1],\\ &\mathfrak{U}(0,t) = \omega_0(t), \qquad \mathfrak{U}(1,t) = \omega_1(t), \qquad t \in [0,1], \end{aligned}$$

where $\kappa_1, \kappa_2 > 0$ are the reaction terms and $\mathcal{D}_{0,t}^{\nu(x,t)}$ is the VO Caputo fractional derivative of order $0 < \nu_{\min} \leq \nu(x,t) \leq \nu_{\max} < 1$ which the order is a continuous function of two variables.

2 | LUCAS WAVELETS AND THEIR PROPERTIES

We now introduce the Lucas wavelets and their properties which shall be utilized in the structure of the method. Lucas wavelet function $\Psi_{nm}(x)$ on the interval $[0,1)$ is defined as follows:[40]

$$\Psi_{nm}(x) = 2^{\frac{\mathcal{K}-1}{2}}\mathcal{L}_m(2^{\mathcal{K}-1}x - n + 1)\chi_{\left[\frac{n-1}{2^{\mathcal{K}-1}}, \frac{n}{2^{\mathcal{K}-1}}\right)}, \tag{3}$$

$$m = 0, 1, \ldots, \mathcal{M}, \qquad n = 1, 2, \ldots, 2^{\mathcal{K}-1},$$

where

$$\mathcal{L}_m(2^{\mathcal{K}-1}x - n + 1) = \frac{1}{\sqrt{\int_0^1 L_m^2(x)dx}}L_m(2^{\mathcal{K}-1}x - n + 1),$$

the coefficient $\frac{1}{\sqrt{\int_0^1 L_m^2(x)dx}}$ in the above formula is for normality, the dilation parameter is $2^{-(\mathcal{K}-1)}$, the translation parameter is $(n-1)2^{-(\mathcal{K}-1)}$ and $\chi_{\left[\frac{n-1}{2^{\mathcal{K}-1}}, \frac{n}{2^{\mathcal{K}-1}}\right)}$ denotes the characteristic function given as

$$\chi_{\left[\frac{n-1}{2^{\mathcal{K}-1}}, \frac{n}{2^{\mathcal{K}-1}}\right)}(x) = \begin{cases} 1, & \frac{n-1}{2^{\mathcal{K}-1}} \leq x < \frac{n}{2^{\mathcal{K}-1}},\\ 0, & \text{otherwise.}\end{cases}$$

And also, the function $L_m(x)$ denotes the Lucas polynomials of degree m defined in $[0,1]$ as follows:[26,27]

$$L_0(x) = 2, \qquad L_m(x) = \sum_{k=0}^{\left[\frac{m}{2}\right]} \frac{m}{m-k}\binom{m-k}{k}x^{m-2k}. \tag{4}$$

The graphs of LWFs for $\mathcal{K} = 2$ with $\mathcal{M} = 3$ are shown in Figure 1.

2.1 | Lucas multiwavelet functions

Here, according to the Lucas wavelet function defined in Equation (3), we present the LMWFs as follows:

$$\Psi_{nm_1m_2}(x,t) = 2^{\mathcal{K}-1}\mathcal{L}_{m_1}(2^{\mathcal{K}-1}x - n + 1)\mathcal{L}_{m_2}(2^{\mathcal{K}-1}t - n + 1)\chi^x_{\left[\frac{n-1}{2^{\mathcal{K}-1}}, \frac{n}{2^{\mathcal{K}-1}}\right)}\chi^t_{\left[\frac{n-1}{2^{\mathcal{K}-1}}, \frac{n}{2^{\mathcal{K}-1}}\right)}, \tag{5}$$

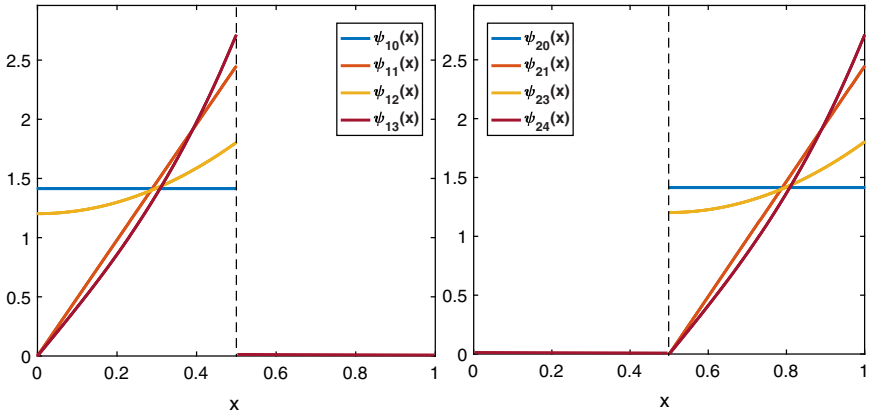

FIGURE 1 The graphs of LWFs for $\mathcal{M} = 3$ and $\mathcal{K} = 2$

$$m_1 = 0, 1, \ldots, \mathcal{M}_1, \quad m_2 = 0, 1, \ldots, \mathcal{M}_2, \quad n = 1, 2, \ldots, 2^{\mathcal{K}-1},$$

where the characteristic functions

$$\chi^x_{\left[\frac{n-1}{2^{\mathcal{K}-1}}, \frac{n}{2^{\mathcal{K}-1}}\right)}(x) = \begin{cases} 1, & \frac{n-1}{2^{\mathcal{K}-1}} \le x < \frac{n}{2^{\mathcal{K}-1}}, \\ 0, & \text{otherwise}, \end{cases}$$

and

$$\chi^t_{\left[\frac{n-1}{2^{\mathcal{K}-1}}, \frac{n}{2^{\mathcal{K}-1}}\right)}(t) = \begin{cases} 1, & \frac{n-1}{2^{\mathcal{K}-1}} \le t < \frac{n}{2^{\mathcal{K}-1}}, \\ 0, & \text{otherwise}, \end{cases}$$

are defined for variables x and t, respectively.

An arbitrary function f defined over $[0,1) \times [0,1)$ can be approximated by terms of the LMWFs as follows:

$$f(x,t) = \sum_{n=1}^{\infty} \sum_{m_1=0}^{\infty} \sum_{m_2=0}^{\infty} a_{nm_1m_2} \Psi_{nm_1m_2}(x,t).$$

The above infinite series can be truncated as follows:

$$f(x,t) \simeq \sum_{n=1}^{2^{\mathcal{K}-1}} \sum_{m_1=0}^{\mathcal{M}_1} \sum_{m_2=0}^{\mathcal{M}_2} a_{nm_1m_2} \Psi_{nm_1m_2}(x,t) = \Psi^T(x) A \Psi(t),$$

where

$$\begin{aligned} A &= [a_{nm_1m_2}]_{2^{\mathcal{K}-1}(\mathcal{M}_1+1) \times 2^{\mathcal{K}-1}(\mathcal{M}_2+1)}, \\ \Psi(x) &= [\Psi_{10}(x), \Psi_{11}(x), \ldots, \Psi_{1\mathcal{M}_1}(x), \ldots, \Psi_{2^{\mathcal{K}-1}0}(x), \Psi_{2^{\mathcal{K}-1}1}(x), \ldots, \Psi_{2^{\mathcal{K}-1}\mathcal{M}_1}(x)]^T, \\ \Psi(t) &= [\Psi_{10}(t), \Psi_{11}(t), \ldots, \Psi_{1\mathcal{M}_2}(t), \ldots, \Psi_{2^{\mathcal{K}-1}0}(t), \Psi_{2^{\mathcal{K}-1}1}(t), \ldots, \Psi_{2^{\mathcal{K}-1}\mathcal{M}_2}(t)]^T. \end{aligned} \tag{6}$$

Each component of the matrix A is determined by the following formula:

$$a_{nm_1m_2} = \langle f(x,t), \Psi_{nm_1m_2}(x,t) \rangle, \quad m_1 = 0, 1, \ldots, \mathcal{M}_1, \quad m_2 = 0, 1, \ldots, \mathcal{M}_2, \quad n = 1, 2, \ldots, 2^{\mathcal{K}-1}.$$

2.2 | Transformation matrix of Lucas wavelets to the Taylor scaling functions

In the following section, to introduce the modified version of the operational matrix, we apply the Taylor scaling functions. These functions are described by the following notation:

$$\Phi_{nm}(x) = x^m \chi_{\left[\frac{n-1}{2^{\mathcal{K}-1}}, \frac{n}{2^{\mathcal{K}-1}}\right)}, \quad m = 0, 1, \ldots, \mathcal{M}, \quad n = 1, 2, \ldots, 2^{\mathcal{K}-1}. \tag{7}$$

By considering LWFs and TSFs, we gain the transformation matrix

$$\Psi(x) = \mathbf{\Theta}\Phi(x), \tag{8}$$

where $\mathbf{\Theta}$ denotes the transformation matrix of LWFs to the TSFs and

$$\Phi(x) = [\Phi_{10}(x), \Phi_{11}(x), \ \dots \ , \Phi_{1\mathcal{M}}(x), \ \dots \ , \Phi_{2^{\mathcal{K}-1}0}(x), \Phi_{2^{\mathcal{K}-1}1}(x), \ \dots \ , \Phi_{2^{\mathcal{K}-1}\mathcal{M}}(x)]^T.$$

For $\mathcal{M} = 2, \mathcal{K} = 2$ the transformation matrix is achieved as follows:[40]

$$\left.\begin{aligned} &\Psi_{10}(x) = \sqrt{2}, \\ &\Psi_{11}(x) = 2\sqrt{6}x, \\ &\Psi_{12}(x) = \tfrac{4\sqrt{30}\sqrt{83}}{83}x^2 + \tfrac{2\sqrt{30}\sqrt{83}}{83}, \end{aligned}\right\}, \quad 0 \le x < \frac{1}{2},$$

and

$$\left.\begin{aligned} &\Psi_{20}(x) = \sqrt{2}, \\ &\Psi_{21}(x) = 2\sqrt{6}x - \sqrt{6}, \\ &\Psi_{22}(x) = \tfrac{4\sqrt{30}\sqrt{83}}{83}x^2 - \tfrac{4\sqrt{30}\sqrt{83}}{83}x + \tfrac{3\sqrt{30}\sqrt{83}}{83}, \end{aligned}\right\} \quad \frac{1}{2} \le x < 1.$$

Therefore, we get

$$\mathbf{\Theta} = \begin{bmatrix} \sqrt{2} & 0 & 0 & 0 & 0 & 0 \\ 0 & 2\sqrt{6} & 0 & 0 & 0 & 0 \\ \frac{2\sqrt{30}\sqrt{83}}{83} & 0 & \frac{4\sqrt{30}\sqrt{83}}{83} & 0 & 0 & 0 \\ 0 & 0 & 0 & \sqrt{2} & 0 & 0 \\ 0 & 0 & 0 & -\sqrt{6} & 2\sqrt{6} & 0 \\ 0 & 0 & 0 & \frac{3\sqrt{30}\sqrt{83}}{83} & \frac{-4\sqrt{30}\sqrt{83}}{83} & \frac{4\sqrt{30}\sqrt{83}}{83} \end{bmatrix}.$$

3 | REQUIREMENT MATRICES

In this part of the study, we present the requirement matrices to apply in the computational approach.

3.1 | MOM of integration for LWFs

In the present section, we describe the method of constructing the MOM of integration. First, we find the MOM of integration for TSFs

$$\int_0^x \Phi(\xi)d\xi = \mathbf{\Upsilon}\Phi(x) + \mathbf{\Delta}(x), \tag{9}$$

where $\mathbf{\Upsilon}$ is MOM of integration for TSFs and $\mathbf{\Delta}(x)$ is the complement vector. From Equation (7), for each component of the TSFs vector, we have

$$\int_0^x \Phi_{nm}(\xi)d\xi = \int_0^x \xi^m \chi_{[\frac{n-1}{2^{\mathcal{K}-1}}, \frac{n}{2^{\mathcal{K}-1}})}d\xi = \begin{cases} 0, & x < \frac{n-1}{2^{\mathcal{K}-1}}, \\ \int_{\frac{n-1}{2^{\mathcal{K}-1}}}^{x} \xi^m d\xi, & \frac{n-1}{2^{\mathcal{K}-1}} \le x \le \frac{n}{2^{\mathcal{K}-1}}, \\ \int_{\frac{n-1}{2^{\mathcal{K}-1}}}^{\frac{n}{2^{\mathcal{K}-1}}} \xi^m d\xi, & \frac{n}{2^{\mathcal{K}-1}} \le x. \end{cases} \tag{10}$$

From $m = 0, 1, \ldots, \mathcal{M}-1$, we obtain

$$\int_0^x \Phi_{nm}(\xi)d\xi = \begin{cases} 0, & x < \frac{n-1}{2^{\mathcal{K}-1}}, \\ \frac{1}{m+1}\left(x^{m+1} - \left(\frac{n-1}{2^{\mathcal{K}-1}}\right)^{m+1}\right), & \frac{n-1}{2^{\mathcal{K}-1}} \le x \le \frac{n}{2^{\mathcal{K}-1}}, \\ \frac{1}{m+1}\left((\frac{n}{2^{\mathcal{K}-1}})^{m+1} - \left(\frac{n-1}{2^{\mathcal{K}-1}}\right)^{m+1}\right), & \frac{n}{2^{\mathcal{K}-1}} \le x, \end{cases}$$
$$= \sum_{i=1}^{2^{\mathcal{K}-1}} \sum_{j=0}^{\mathcal{M}} c_{ij}^{nm} \Phi_{ij}(x). \tag{11}$$

For $m = \mathcal{M}$, we get

$$\int_0^x \Phi_{n\mathcal{M}}(\xi)d\xi = \begin{cases} 0, & x < \frac{n-1}{2^{\mathcal{K}-1}}, \\ \frac{1}{\mathcal{M}+1}\left(x^{\mathcal{M}+1} - \left(\frac{n-1}{2^{\mathcal{K}-1}}\right)^{\mathcal{M}+1}\right), & \frac{n-1}{2^{\mathcal{K}-1}} \le x \le \frac{n}{2^{\mathcal{K}-1}}, \\ \frac{1}{\mathcal{M}+1}\left(\left(\frac{n}{2^{\mathcal{K}-1}}\right)^{\mathcal{M}+1} - \left(\frac{n-1}{2^{\mathcal{K}-1}}\right)^{\mathcal{M}+1}\right), & \frac{n}{2^{\mathcal{K}-1}} \le x, \end{cases}$$
$$= \sum_{i=1}^{2^{k-1}} \sum_{j=0}^{\mathcal{M}} d_{ij}^{n} \Phi_{ij}(x) + \Delta_{\mathcal{M}}^{n}(x). \tag{12}$$

Therefore, the proposed matrix and vector have the following form:

$$\boldsymbol{\Upsilon} = \begin{bmatrix} c_{10}^{10} & c_{11}^{10} & \cdots & c_{1\mathcal{M}}^{10} & \cdots & c_{2^{\mathcal{K}-1}0}^{10} & c_{2^{\mathcal{K}-1}1}^{10} & \cdots & c_{2^{\mathcal{K}-1}\mathcal{M}}^{10} \\ \vdots & \vdots & \ddots & \vdots & \ddots & \vdots & \vdots & \ddots & \vdots \\ d_{10}^{1} & d_{11}^{1} & \cdots & d_{1\mathcal{M}}^{1} & \cdots & d_{2^{\mathcal{K}-1}0}^{1} & d_{2^{\mathcal{K}-1}1}^{1} & \cdots & d_{2^{\mathcal{K}-1}\mathcal{M}}^{1} \\ \vdots & \vdots & \ddots & \vdots & \ddots & \vdots & \vdots & \ddots & \vdots \\ c_{10}^{2^{\mathcal{K}-1}0} & c_{11}^{2^{\mathcal{K}-1}0} & \cdots & c_{1\mathcal{M}}^{2^{\mathcal{K}-1}0} & \cdots & c_{2^{\mathcal{K}-1}0}^{2^{\mathcal{K}-1}0} & c_{2^{\mathcal{K}-1}1}^{2^{\mathcal{K}-1}0} & \cdots & c_{2^{\mathcal{K}-1}\mathcal{M}}^{2^{\mathcal{K}-1}0} \\ \vdots & \vdots & \ddots & \vdots & \ddots & \vdots & \vdots & \ddots & \vdots \\ d_{10}^{2^{\mathcal{K}-1}} & d_{11}^{2^{\mathcal{K}-1}} & \cdots & d_{1\mathcal{M}}^{2^{\mathcal{K}-1}} & \cdots & d_{2^{\mathcal{K}-1}0}^{2^{\mathcal{K}-1}} & d_{2^{\mathcal{K}-1}1}^{2^{\mathcal{K}-1}} & \cdots & d_{2^{\mathcal{K}-1}\mathcal{M}}^{2^{\mathcal{K}-1}} \end{bmatrix},$$

and

$$\boldsymbol{\Delta}(x) = [\boldsymbol{\Delta}_{n,m}(x)], \quad \boldsymbol{\Delta}_{n,m}(x) = \begin{cases} \Delta_{\mathcal{M}}^{n}(x), & m = \mathcal{M}, \\ 0, & m = 0, 1, \ldots, \mathcal{M}-1, \end{cases} \quad n = 1, 2, \ldots, 2^{\mathcal{K}-1}.$$

Now, with the help of MOM of integration for TSFs and transformation matrix can be obtained MOM of integration for LWFs. Hence, from Equations (8) and (9), we deduce

$$\int_0^x \Psi(\xi)d\xi = \int_0^x \boldsymbol{\Theta}\Phi(\xi)d\xi = \boldsymbol{\Theta}(\boldsymbol{\Upsilon}\Phi(x) + \boldsymbol{\Delta}(x)) = \boldsymbol{\Theta}(\boldsymbol{\Upsilon}\boldsymbol{\Theta}^{-1}\Psi(x) + \boldsymbol{\Delta}(x))$$
$$= \boldsymbol{\Theta}\boldsymbol{\Upsilon}\boldsymbol{\Theta}^{-1}\Psi(x) + \boldsymbol{\Theta}\boldsymbol{\Delta}(x) = \mathbf{Q}\Psi(x) + \boldsymbol{\Lambda}(x). \tag{13}$$

Here, $\mathbf{Q}$ denotes the MOM of integration and $\boldsymbol{\Lambda}(x)$ is called the complement vector for LWFs. Another remarkable fact is that we can write the above procedure for the variable t as follows:

$$\int_0^t \Psi(\eta)d\eta = \tilde{\mathrm{Q}}\Psi(t) + \tilde{\boldsymbol{\Lambda}}(t). \tag{14}$$

3.2 | POM of VO fractional derivative

In this section, to describe the process of calculating the POM of VO-fractional derivative for LWFs, we use the transformation matrix and the POM of VO-fractional derivative for TSFs given below:

$$\mathcal{D}_t^{\nu(x,t)}\Phi(t) \simeq t^{-\nu(x,t)}\mathbf{D}\Phi(t), \tag{15}$$

where $\mathbf{D}$ is the POM of VO-fractional derivative for TSFs. Now, by using Equation (7), we conclude

$$\begin{aligned}\mathcal{D}_t^{\nu(x,t)}\Phi_{nm}(t) &= \mathcal{D}_t^{\nu(x,t)}\left(t^m \chi_{[\frac{n-1}{2^{\mathcal{K}-1}},\frac{n}{2^{\mathcal{K}-1}})}\right)\\ &= \frac{1}{\Gamma(1-\nu(x,t))}\left(\int_{\frac{n-1}{2^{\mathcal{K}-1}}}^{\frac{n}{2^{\mathcal{K}-1}}} \frac{\frac{d}{dx}x^m}{(t-x)^{\nu(x,t)}}dx + \int_{\frac{n}{2^{\mathcal{K}-1}}}^{t} \frac{\frac{d}{dx}x^m}{(t-x)^{\nu(x,t)}}dx\right)\\ &= t^{-\nu(x,t)}\sum_{i=1}^{2^{\mathcal{K}-1}}\sum_{j=0}^{\mathcal{M}} a_{ij}^{nm}\Phi_{ij}(t).\end{aligned} \tag{16}$$

Then, in view of the above relations the compact form of VO-fractional derivative of LWFs is obtained as follows:

$$\begin{aligned}\mathcal{D}_t^{\nu(x,t)}\Psi(t) &= \mathbf{\Theta}\mathcal{D}_t^{\nu(x,t)}\Phi(t) = t^{-\nu(x,t)}\mathbf{\Theta}\mathbf{D}\Phi(t)\\ &= t^{-\nu(x,t)}\mathbf{\Theta}\mathbf{D}\mathbf{\Theta}^{-1}\Psi(t)\\ &= t^{-\nu(x,t)}\mathbf{R}\Psi(t).\end{aligned} \tag{17}$$

Here, $\mathbf{R}$ is called POM of VO-fractional derivative for LWFs.

4 | DESCRIPTION OF THE NUMERICAL TECHNIQUE

In this section, the algorithm for determining the approximate solution based on the operational matrices and LMWFs is presented. Now, to approximate the functions, we assume that

$$\frac{\partial^3 \mathfrak{U}(x,t)}{\partial x^2 \partial t} \simeq \Psi^T(x)\mathbf{U}\Psi(t). \tag{18}$$

By successively integrating the above expression with respect to the component t and x, respectively, we obtain:

$$\frac{\partial^2 \mathfrak{U}(x,t)}{\partial x^2} \simeq \Psi^T(x)\mathbf{U}(\tilde{\mathbf{Q}}\Psi(t) + \tilde{\boldsymbol{\Lambda}}(t)) + \varphi''(x), \tag{19}$$

and

$$\frac{\partial \mathfrak{U}(x,t)}{\partial x} \simeq (\Psi^T(x)\mathbf{Q}^T + \mathbf{\Lambda}^T(x))\mathbf{U}(\tilde{\mathbf{Q}}\Psi(t) + \tilde{\boldsymbol{\Lambda}}(t)) + \varphi'(x) - \varphi'(0) + \left.\frac{\partial \mathfrak{U}(x,t)}{\partial x}\right|_{x=0}. \tag{20}$$

Before computing the approximation of the other functions, we approximate the unknown function $\left.\frac{\partial \mathfrak{U}(x,t)}{\partial x}\right|_{x=0}$ by integrating Equation (20) from 0 to 1:

$$\left.\frac{\partial \mathfrak{U}(x,t)}{\partial x}\right|_{x=0} \simeq \omega_1(t) - \omega_0(t) - \left(\left[\int_0^1 \Psi^T(x)dx\right]\mathbf{Q}^T + \int_0^1 \mathbf{\Lambda}^T(x)dx\right)\mathbf{U}(\tilde{\mathbf{Q}}\Psi(t) + \tilde{\boldsymbol{\Lambda}}(t)) + \varphi(1) - \varphi(0) - \varphi'(0). \tag{21}$$

Then, in view of two recent relations, we conclude:

$$\mathfrak{U}(x,t) \simeq (\Psi^T(x)(\mathbf{Q}^T)^2 + \mathbf{\Lambda}^T(x)\mathbf{Q}^T + \mathbf{J}^T(x))\mathbf{U}(\tilde{\mathbf{Q}}\Psi(t) + \tilde{\boldsymbol{\Lambda}}(t)) + \varphi(x) - \varphi(0) - x\varphi'(0) + x\left.\frac{\partial \mathfrak{U}(x,t)}{\partial x}\right|_{x=0} + \omega_0(t). \tag{22}$$

where

$$\mathbf{J}(x) = \int_0^x \mathbf{\Lambda}(\xi)d\xi.$$

By integrating Equation (18) with respect to the component x, we gain:

$$\frac{\partial^2 \mathfrak{U}(x,t)}{\partial x \partial t} \simeq (\Psi^T(x)\mathbf{Q}^T + \mathbf{\Lambda}^T(x))\mathbf{U}\Psi(t) + \left.\frac{\partial^2 \mathfrak{U}(x,t)}{\partial x \partial t}\right|_{x=0}. \tag{23}$$

Before we go on, by integrating Equation (23) with respect to x from 0 to 1, we get

$$\left.\frac{\partial^2 \mathfrak{U}(x,t)}{\partial x \partial t}\right|_{x=0} \simeq \omega_1'(t) - \omega_0'(t) - \left(\left[\int_0^1 \Psi^T(x)dx\right]\mathbf{Q}^T + \int_0^1 \mathbf{\Lambda}^T(x)dx\right)\mathbf{U}\Psi(t). \tag{24}$$

As the integration process continues, we have:

$$\frac{\partial \mathfrak{U}(x,t)}{\partial t} \simeq (\Psi^T(x)(\mathbf{Q}^T)^2 + \mathbf{\Lambda}^T(x)\mathbf{Q}^T + \mathbf{J}^T(x))\mathbf{U}\Psi(t) + x\left.\frac{\partial^2 \mathfrak{U}(x,t)}{\partial x \partial t}\right|_{x=0} + \omega_0'(t). \tag{25}$$

Next, by applying the VO Caputo fractional derivative into Equations (19) and (22), we approximate the VO-fractional derivative part of these equations, respectively. Hence, we get

$$\begin{aligned}\mathcal{D}_{0,t}^{\nu(t)}\mathfrak{U}(x,t) \simeq{}& (\Psi^T(x)(\mathbf{Q}^T)^2 + \mathbf{\Lambda}^T(x)\mathbf{Q}^T + \mathbf{J}^T(x))\mathbf{U}(t^{-\nu(t)}\tilde{\mathbf{Q}}\mathbf{R}\Psi(t) + \mathcal{D}_{0,t}^{\nu(t)}\tilde{\mathbf{\Lambda}}(t))\\ &+ x\mathcal{D}_{0,t}^{\nu(t)}\left(\left.\frac{\partial \mathfrak{U}(x,t)}{\partial x}\right|_{x=0}\right) + \mathcal{D}_{0,t}^{\nu(t)}\omega_0(t),\end{aligned} \tag{26}$$

where

$$\begin{aligned}\mathcal{D}_{0,t}^{\nu(t)}\left(\left.\frac{\partial \mathfrak{U}(x,t)}{\partial x}\right|_{x=0}\right) \simeq{}& -\left(\left[\int_0^1 \Psi^T(x)dx\right]\mathbf{Q}^T + \int_0^1 \mathbf{\Lambda}^T(x)dx\right)\mathbf{U}(t^{-\nu(t)}\tilde{\mathbf{Q}}\mathbf{R}\Psi(t) + \mathcal{D}_{0,t}^{\nu(t)}\tilde{\mathbf{\Lambda}}(t))\\ &+ \mathcal{D}_{0,t}^{\nu(t)}\omega_1(t) - \mathcal{D}_{0,t}^{\nu(t)}\omega_0(t).\end{aligned} \tag{27}$$

And also, we obtain

$$\mathcal{D}_{0,t}^{1-\nu(x,t)}\left(\frac{\partial^2 \mathfrak{U}(x,t)}{\partial x^2}\right) \simeq \Psi^T(x)\mathbf{U}(t^{1-\nu(x,t)}\tilde{\mathbf{Q}}\mathbf{R}\Psi(t) + \mathcal{D}_{0,t}^{1-\nu(x,t)}\tilde{\mathbf{\Lambda}}(t)). \tag{28}$$

Consequently, by replacing the approximation functions obtained in proposed problems, we obtain
Problem 1:

$$\begin{aligned}\mathbf{\Psi}(x,t,\mathbf{U}) ={}& (\Psi^T(x)(\mathbf{Q}^T)^2 + \mathbf{\Lambda}^T(x)\mathbf{Q}^T + \mathbf{J}^T(x))\mathbf{U}(t^{-\nu(t)}\tilde{\mathbf{Q}}\mathbf{R}\Psi(t) + \mathcal{D}_{0,t}^{\nu(t)}\tilde{\mathbf{\Lambda}}(t))\\ &+ x\left[-\left(\left[\int_0^1 \Psi^T(x)dx\right]\mathbf{Q}^T + \int_0^1 \mathbf{\Lambda}^T(x)dx\right)\mathbf{U}(t^{-\nu(t)}\tilde{\mathbf{Q}}\mathbf{R}\Psi(t) + \mathcal{D}_{0,t}^{\nu(t)}\tilde{\mathbf{\Lambda}}(t))\right.\\ &\left. + \mathcal{D}_{0,t}^{\nu(t)}\omega_1(t) - \mathcal{D}_{0,t}^{\nu(t)}\omega_0(t)\right] + \mathcal{D}_{0,t}^{\nu(t)}\omega_0(t) - \kappa[\Psi^T(x)\mathbf{U}(\tilde{\mathbf{Q}}\Psi(t) + \tilde{\mathbf{\Lambda}}(t)) + \varphi''(x)]\\ &+ \mathcal{F}\left(x,t,(\Psi^T(x)(\mathbf{Q}^T)^2 + \mathbf{\Lambda}^T(x)\mathbf{Q}^T + \mathbf{J}^T(x))\mathbf{U}(\tilde{\mathbf{Q}}\Psi(t) + \tilde{\mathbf{\Lambda}}(t)) + \varphi(x) - \varphi(0) - x\varphi'(0)\right.\\ &+ x\left[-\left(\left[\int_0^1 \Psi^T(x)dx\right]\mathbf{Q}^T + \int_0^1 \mathbf{\Lambda}^T(x)dx\right)\mathbf{U}(t^{-\nu(t)}\tilde{\mathbf{Q}}\mathbf{R}\Psi(t) + \mathcal{D}_{0,t}^{\nu(t)}\tilde{\mathbf{\Lambda}}(t))\right.\\ &\left.\left. + \mathcal{D}_{0,t}^{\nu(t)}\omega_1(t) - \mathcal{D}_{0,t}^{\nu(t)}\omega_0(t)\right] + \omega_0(t)\right) = 0.\end{aligned} \tag{29}$$

Problem 2:

$$\begin{aligned}\mathbf{\Pi}(x,t,\mathbf{U}) ={}& (\Psi^T(x)(\mathbf{Q}^T)^2 + \mathbf{\Lambda}^T(x)\mathbf{Q}^T + \mathbf{J}^T(x))\mathbf{U}\Psi(t) + x\left.\frac{\partial^2 \mathfrak{U}(x,t)}{\partial x \partial t}\right|_{x=0} + \omega_0'(t)\\ &- \kappa_1[\Psi^T(x)\mathbf{U}(t^{1-\nu(x,t)}\tilde{\mathbf{Q}}\mathbf{R}\Psi(t) + \mathcal{D}_{0,t}^{1-\nu(x,t)}\tilde{\mathbf{\Lambda}}(t))]\\ &+ \kappa_2\left[(\Psi^T(x)(\mathbf{Q}^T)^2 + \mathbf{\Lambda}^T(x)\mathbf{Q}^T + \mathbf{J}^T(x))\mathbf{U}(t^{-\nu(x,t)}\tilde{\mathbf{Q}}\mathbf{R}\Psi(t) + \mathcal{D}_{0,t}^{\nu(x,t)}\tilde{\mathbf{\Lambda}}(t))\right.\end{aligned}$$

$$
\begin{aligned}
&+ x\left[-\left(\left[\int_0^1 \Psi^T(x)dx\right]\mathbf{Q}^T + \int_0^1 \mathbf{\Lambda}^T(x)dx\right)\mathbf{U}(t^{-\nu(x,t)}\tilde{\mathbf{Q}}\mathbf{R}\Psi(t) + \mathcal{D}_{0,t}^{\nu(x,t)}\tilde{\mathbf{\Lambda}}(t))\right.\\
&\left.+\ \mathcal{D}_{0,t}^{\nu(x,t)}\omega_1(t) - \mathcal{D}_{0,t}^{\nu(x,t)}\omega_0(t)\right] + \mathcal{D}_{0,t}^{\nu(x,t)}\omega_0(t)\Big]\\
&- \mathcal{G}\left(x, t, (\Psi^T(x)(\mathbf{Q}^T)^2 + \mathbf{\Lambda}^T(x)\mathbf{Q}^T + \mathbf{J}^T(x))\mathbf{U}(\tilde{\mathbf{Q}}\Psi(t) + \tilde{\mathbf{\Lambda}}(t)) + \varphi(x) - \varphi(0) - x\varphi'(0)\right.\\
&+ x\left[\omega_1(t) - \omega_0(t) - \left(\left[\int_0^1 \Psi^T(x)dx\right]\mathbf{Q}^T + \int_0^1 \mathbf{\Lambda}^T(x)dx\right)\mathbf{U}(\tilde{\mathbf{Q}}\Psi(t) + \tilde{\mathbf{\Lambda}}(t))\right.\\
&\left.\left.+\ \varphi(1) - \varphi(0) - \varphi'(0)\right] + \omega_0(t)\right) = 0.
\end{aligned}
\tag{30}
$$

By substituting $2^{\mathcal{K}-1}(\mathcal{M}_1+1)$ and $2^{\mathcal{K}-1}(\mathcal{M}_2+1)$ the nodal points of Newton–Cotes:[41]

$$
x_i = \frac{2i-1}{2^{\mathcal{K}}(\mathcal{M}_1+1)}, \quad t_j = \frac{2j-1}{2^{\mathcal{K}}(\mathcal{M}_2+1)}, \quad i = 1, 2, \ldots, 2^{\mathcal{K}-1}(\mathcal{M}_1+1), \quad j = 1, 2, \ldots, 2^{\mathcal{K}-1}(\mathcal{M}_2+1),
$$

into variables x and t, respectively, in the aforementioned formulas, we get the following system of algebraic equations

$$
\mathbf{\Psi}(x_i, t_j, \mathbf{U}) = 0, \qquad \mathbf{\Pi}(x_i, t_j, \mathbf{U}) = 0, \quad i = 1, 2, \ldots, 2^{\mathcal{K}-1}(\mathcal{M}_1+1), \quad j = 1, 2, \ldots, 2^{\mathcal{K}-1}(\mathcal{M}_2+1).
$$

Therefore, we can obtain the unknown matrix U and also the approximate solution with the help of Newton's iterative method.

5 | CONVERGENCE ANALYSIS

This section considered an estimation error bound of an approximate solution obtained by the proposed method.

Lemma 1. *For any nonnegative integer m, we have the identities*[42]

$$
x^m = \sum_{k=0}^{m} \frac{(-1)^{\frac{m-k}{2}}\delta_k(\frac{m+k}{2}+1)_{\frac{m-k}{2}}}{(\frac{m-k}{2})!}L_k(x), \tag{31}
$$

where $(a)_b = \frac{\Gamma(a+b)}{\Gamma(a)}$ *is Pochhammer notation and*

$$
\delta_k = \begin{cases} \frac{1}{2}, & k = 0, \\ 1, & k > 0. \end{cases}
$$

Lemma 2. *Assume that the function $f(x)$ is infinitely differentiable on the interval $[0,1]$, then the expansion of the function in terms of Lucas polynomials is Reference* 43

$$
f(x) = \sum_{k=0}^{\infty} c_k L_k(x), \qquad c_k = \sum_{j=0}^{\infty} \frac{(-1)^j \delta_k f^{(k+2j)}(0)}{j!(k+j)!}. \tag{32}
$$

Lemma 3. *Let $f_n : (\frac{n-1}{2^{\mathcal{K}-1}}, \frac{n}{2^{\mathcal{K}-1}}) \to R$ is a function in $L^2(\frac{n-1}{2^{\mathcal{K}-1}}, \frac{n}{2^{\mathcal{K}-1}})$.Consider the function $F_n f_n : (0,1) \to R$ such that $F_n f_n(s) = f_n(\frac{1}{2^{\mathcal{K}-1}}(s+n-1))$ for all $s \in (0,1)$, then we have*

$$
\|F_n f_n\|_{L^2(0,1)} = 2^{\frac{1}{2}(\mathcal{K}-1)}\|f_n\|_{L^2(\frac{n-1}{2^{\mathcal{K}-1}}, \frac{n}{2^{\mathcal{K}-1}})}. \tag{33}
$$

Proof. With the help of a change of variable $x = \frac{1}{2^{\mathcal{K}-1}}(s+n-1)$, we get

$$
\begin{aligned}
\|F_n f_n\|^2_{L^2(0,1)} &= \int_0^1 |F_n f_n(s)|^2 ds = \int_0^1 |f_n(\frac{1}{2^{\mathcal{K}-1}}(s+n-1))|^2 ds\\
&= \int_{\frac{n-1}{2^{\mathcal{K}-1}}}^{\frac{n}{2^{\mathcal{K}-1}}} 2^{\mathcal{K}-1}|f_n(x)|^2 dx = 2^{\mathcal{K}-1}\|f_n\|^2_{L^2(\frac{n-1}{2^{\mathcal{K}-1}}, \frac{n}{2^{\mathcal{K}-1}})}.
\end{aligned}
\tag{34}
$$

By taking the square roots of both sides of Equation (34), the desired result is achieved. ∎

Theorem 1. *Let $\mathcal{P}_f(x) = \sum_{k=0}^{\mathcal{M}_1} c_k L_k(x)$ be approximate of the function $f(x)$, then the error estimate $\mathcal{E}_{\mathcal{M}_1} = f(x) - \mathcal{P}_f(x)$ is obtained as:*

$$\|\mathcal{E}_{\mathcal{M}_1}\|_{L_2[0,1]} \leq \left[\sum_{j=0}^{\infty} \frac{\delta_{\mathcal{M}_1+1}^2 \mathcal{R}_{\mathcal{M}_1+1}}{(j!)^2(\mathcal{M}_1+1+j)!^2} (\sup_{x\in[0,1]} |f^{(\mathcal{M}_1+1+2j)}(0)|)^2\right]^{\frac{1}{2}}. \tag{35}$$

Here,

$$\mathcal{R}_{\mathcal{M}_1+1} = \int_0^1 L_{\mathcal{M}_1+1}^2(x)dx.$$

Proof. Due to Equation (32), we can write

$$|f(x) - \mathcal{P}_f(x)| \leq \sum_{j=0}^{\infty} \frac{\delta_{\mathcal{M}_1+1} L_{\mathcal{M}_1+1}(x)}{j!(\mathcal{M}_1+1+j)!} \sup_{x\in[0,1]} |f^{(\mathcal{M}_1+1+2j)}(0)|.$$

Therefore, we have

$$\begin{aligned}
\|\mathcal{E}_{\mathcal{M}_1}\|_{L_2[0,1]}^2 &= \int_0^1 |f(x) - \mathcal{P}_f(x)|^2 dx \\
&\leq \int_0^1 \left[\sum_{j=0}^{\infty} \frac{\delta_{\mathcal{M}_1+1} L_{\mathcal{M}_1+1}(x)}{j!(\mathcal{M}_1+1+j)!} \sup_{x\in[0,1]} |f^{(\mathcal{M}_1+1+2j)}(0)|\right]^2 dx \\
&\leq \sum_{j=0}^{\infty} \frac{\delta_{\mathcal{M}_1+1}^2}{(j!)^2(\mathcal{M}_1+1+j)!^2} (\sup_{x\in[0,1]} |f^{(\mathcal{M}_1+1+2j)}(0)|)^2 \left[\int_0^1 L_{\mathcal{M}_1+1}^2(x)dx\right].
\end{aligned} \tag{36}$$

In addition, from Equation (4), can be written

$$\int_0^1 L_{\mathcal{M}_1+1}^2(x)dx = \int_0^1 \left(\sum_{r=0}^{[\frac{\mathcal{M}_1+1}{2}]} \frac{(\mathcal{M}_1+1)}{(\mathcal{M}_1+1-r)} \binom{\mathcal{M}_1+1-r}{r} x^{\mathcal{M}_1+1-2r}\right)^2 dx = \mathcal{R}_{\mathcal{M}_1+1}. \tag{37}$$

Accordingly, from Equations (36) to (37), we conclude

$$\|\mathcal{E}_{\mathcal{M}_1}\|_{L_2[0,1]}^2 \leq \sum_{j=0}^{\infty} \frac{\delta_{\mathcal{M}_1+1}^2 \mathcal{R}_{\mathcal{M}_1+1}}{(j!)^2(\mathcal{M}_1+1+j)!^2} (\sup_{x\in[0,1]} |f^{(\mathcal{M}_1+1+2j)}(0)|)^2. \tag{38}$$

∎

Theorem 2. *Suppose that $F_{\mathcal{M}_2}$ and $F_{\mathcal{M}_1}$ are sufficiently smooth functions on region Ω, so that*

$$F_{\mathcal{M}_2}(x,t) = \sum_{n=1}^{2^{\mathcal{K}-1}} \sum_{m_1=0}^{\infty} a_{n,m_1,\mathcal{M}_2} \Psi_{nm_1}(x) \Psi_{n\mathcal{M}_2}(t), \qquad F_{\mathcal{M}_1}(x,t) = \sum_{n=1}^{2^{\mathcal{K}-1}} \sum_{m_2=0}^{\infty} a_{n,\mathcal{M}_1,m_2} \Psi_{n\mathcal{M}_1}(x) \Psi_{nm_2}(t),$$

which are approximated by the following two functions:

$$F_{m_1,\mathcal{M}_2}(x,t) = \sum_{n=1}^{2^{\mathcal{K}-1}} \sum_{m_1=0}^{\mathcal{M}_1} a_{n,m_1,\mathcal{M}_2} \Psi_{nm_1}(x) \Psi_{n\mathcal{M}_2}(t), \qquad F_{m_2,\mathcal{M}_1}(x,t) = \sum_{n=1}^{2^{\mathcal{K}-1}} \sum_{m_2=0}^{\mathcal{M}_2} a_{n,\mathcal{M}_1,m_2} \Psi_{n\mathcal{M}_1}(x) \Psi_{nm_2}(t).$$

Then, the upper bound of error is calculated as follows:

$$\|F_{\mathcal{M}_2} - F_{m_1,\mathcal{M}_2}\|_{L^2(\Omega)} \leq \sum_{n=1}^{2^{k-1}} \left[\sum_{j=0}^{\infty} \frac{\delta_{\mathcal{M}_1+1}^2 \mathcal{R}_{\mathcal{M}_1+1}}{(j!)^2(\mathcal{M}_1+1+j)!^2} (\sup_{x\in[0,1]} |f^{(\mathcal{M}_1+1+2j)}(0)|)^2\right]^{\frac{1}{2}}, \tag{39}$$

and

$$\|F_{\mathcal{M}_1} - F_{m_2,\mathcal{M}_1}\|_{L^2(\Omega)} \leq \sum_{n=1}^{2^{k-1}} \left[\sum_{j=0}^{\infty} \frac{\delta^2_{\mathcal{M}_2+1} \mathcal{R}_{\mathcal{M}_2+1}}{(j!)^2(\mathcal{M}_2+1+j)!^2} (\sup_{x\in[0,1]} |f^{(\mathcal{M}_2+1+2j)}(0)|)^2 \right]^{\frac{1}{2}}. \tag{40}$$

Proof. According to the functions defined above, we can write:

$$\begin{aligned}
\|F_{\mathcal{M}_2} - F_{m_1,\mathcal{M}_2}\|_{L^2(\Omega)} &= \left\| \sum_{n=1}^{2^{\mathcal{K}-1}} \sum_{m_1=0}^{\infty} a_{n,m_1,\mathcal{M}_2} \Psi_{nm_1} \Psi_{n\mathcal{M}_2} - \sum_{n=1}^{2^{\mathcal{K}-1}} \sum_{m_1=0}^{\mathcal{M}_1} a_{n,m_1,\mathcal{M}_2} \Psi_{nm_1} \Psi_{n\mathcal{M}_2} \right\|_{L^2(\Omega)} \\
&= \left\| \left[\sum_{n=1}^{2^{\mathcal{K}-1}} \sum_{m_1=0}^{\infty} a_{n,m_1,\mathcal{M}_2} \Psi_{nm_1} - \sum_{n=1}^{2^{\mathcal{K}-1}} \sum_{m_1=0}^{\mathcal{M}_1} a_{n,m_1,\mathcal{M}_2} \Psi_{nm_1} \right] \Psi_{n\mathcal{M}_2} \right\|_{L^2(\Omega)} \\
&= \left\| \sum_{n=1}^{2^{\mathcal{K}-1}} \sum_{m_1=0}^{\infty} a_{n,m_1,\mathcal{M}_2} \Psi_{nm_1} - \sum_{n=1}^{2^{\mathcal{K}-1}} \sum_{m_1=0}^{\mathcal{M}_1} a_{n,m_1,\mathcal{M}_2} \Psi_{nm_1} \right\|_{L^2[0,1]} \left\| \sum_{n=1}^{2^{\mathcal{K}-1}} \Psi_{n\mathcal{M}_2} \right\|_{L^2[0,1]} \\
&= \sum_{n=1}^{2^{\mathcal{K}-1}} \left\| \sum_{m_1=0}^{\infty} c_{m_1} L_{m_1} - \sum_{m_1=0}^{\mathcal{M}_1} c_{m_1} L_{m_1} \right\|_{L^2(\frac{n-1}{2^{\mathcal{K}-1}}, \frac{n}{2^{\mathcal{K}-1}})} \left\| \sum_{n=1}^{2^{\mathcal{K}-1}} \Psi_{n\mathcal{M}_2} \right\|_{L^2(0,1)} \\
&= 2^{\frac{-1}{2}(\mathcal{K}-1)} \sum_{n=1}^{2^{\mathcal{K}-1}} \|f - \mathcal{P}_f\|_{L^2(0,1)} \left\| \sum_{n=1}^{2^{\mathcal{K}-1}} \Psi_{n\mathcal{M}_2} \right\|_{L^2(0,1)} \\
&= 2^{\frac{-1}{2}(\mathcal{K}-1)} \sum_{n=1}^{2^{\mathcal{K}-1}} \|\mathcal{E}_{\mathcal{M}_1}\|_{L^2(0,1)} \left\| \sum_{n=1}^{2^{\mathcal{K}-1}} \Psi_{n\mathcal{M}_2} \right\|_{L^2(0,1)} \\
&\leq 2^{\frac{-1}{2}(\mathcal{K}-1)} \sum_{n=1}^{2^{\mathcal{K}-1}} \left[\sum_{j=0}^{\infty} \frac{\delta^2_{\mathcal{M}_1+1} \mathcal{R}_{\mathcal{M}_1+1}}{(j!)^2(\mathcal{M}_1+1+j)!^2} (\sup_{x\in[0,1]} |f^{(\mathcal{M}_1+1+2j)}(0)|)^2 \right]^{\frac{1}{2}} \left\| \sum_{n=1}^{2^{\mathcal{K}-1}} \Psi_{n\mathcal{M}_2} \right\|_{L^2(0,1)}.
\end{aligned} \tag{41}$$

On the other hand, we have:

$$\begin{aligned}
\left\| \sum_{n=1}^{2^{\mathcal{K}-1}} \Psi_{n\mathcal{M}_2} \right\|_{L^2(0,1)} &= \left(\int_0^1 \left| \sum_{n=1}^{2^{\mathcal{K}-1}} \Psi_{n\mathcal{M}_2}(t) \right|^2 dt \right)^{\frac{1}{2}} \leq \left(\int_0^1 \sum_{n=1}^{2^{\mathcal{K}-1}} |\Psi_{n\mathcal{M}_2}(t)|^2 dt \right)^{\frac{1}{2}} \\
&= \left(\sum_{n=1}^{2^{\mathcal{K}-1}} \int_0^1 |\Psi_{n\mathcal{M}_2}(t)|^2 dt \right)^{\frac{1}{2}} = 2^{\frac{1}{2}(\mathcal{K}-1)}
\end{aligned} \tag{42}$$

As a result, from Equations (41) to (42), the proof is completed. It must be pointed out that similar to the above process, we can prove Equation (40). ∎

6 | NUMERICAL EXPERIMENTS

In the current section, we investigate some test problems to examine the accuracy and capability of the proposed numerical scheme. All computations are carried out in MATLAB software. It is worth mentioning that to demonstrate the accuracy of the method, we present L_2 and L_∞ errors

$$L_2 = \left(\sum_{i=1}^{\mathcal{M}_1 2^{\mathcal{K}-1}} \sum_{j=1}^{\mathcal{M}_2 2^{\mathcal{K}-1}} |u(x_i,t_j) - u_{\mathcal{M}_1\mathcal{M}_2}(x_i,t_j)|^2 \right)^{\frac{1}{2}},$$

$$L_\infty = \max_{1\leq i\leq \mathcal{M}_1 2^{\mathcal{K}-1}, 1\leq j\leq \mathcal{M}_2 2^{\mathcal{K}-1}} |u(x_i,t_j) - u_{\mathcal{M}_1\mathcal{M}_2}(x_i,t_j)|.$$

TABLE 1 The obtained absolute error of the proposed method for different choices of $\nu(t)$ with $\mathcal{M}_1 = 3, \mathcal{M}_2 = 4$, and $\mathcal{K} = 1$ of Example 1

$x = t$	$\nu(t) = 0.25$	$\nu(t) = 0.5$	$\nu(t) = 0.75$	$\nu(t) = 1$
0	0	0	0	0
0.1	2.5076×10^{-8}	1.1614×10^{-7}	2.0600×10^{-7}	2.7663×10^{-16}
0.2	2.1020×10^{-6}	2.7115×10^{-6}	1.9820×10^{-6}	1.5218×10^{-16}
0.3	6.6431×10^{-7}	1.8503×10^{-6}	2.6123×10^{-6}	8.5662×10^{-16}
0.4	6.3902×10^{-7}	2.5090×10^{-6}	3.9027×10^{-6}	4.4569×10^{-15}
0.5	3.0375×10^{-9}	9.7053×10^{-9}	1.8301×10^{-8}	1.1314×10^{-14}
0.6	6.7067×10^{-6}	1.4795×10^{-5}	1.7715×10^{-5}	1.9983×10^{-14}
0.7	1.5374×10^{-5}	3.4981×10^{-5}	4.2337×10^{-5}	2.8895×10^{-14}
0.8	1.5868×10^{-5}	3.9460×10^{-5}	4.9929×10^{-5}	3.5558×10^{-14}
0.9	1.1296×10^{-5}	2.4642×10^{-5}	2.9277×10^{-5}	3.0729×10^{-14}
1	2.9387×10^{-39}	1.2489×10^{-38}	1.8367×10^{-39}	3.6734×10^{-39}

TABLE 2 The obtained absolute error of the proposed method for different choices of $\nu(t)$ and $\mathcal{M}_2$ with $\mathcal{M}_1 = 3$ and $\mathcal{K} = 1$ of Example 1

	$\nu(t) = \frac{2+\sin(t)}{400}$		$\nu(t) = \frac{20\exp(\frac{t}{2})-12}{20\exp(\frac{t}{2})-10}$	
	$\mathcal{M}_2 = 4$	$\mathcal{M}_2 = 6$	$\mathcal{M}_2 = 4$	$\mathcal{M}_2 = 6$
L_∞-error	1.7228×10^{-7}	1.6931×10^{-7}	3.9337×10^{-5}	6.7897×10^{-6}

6.1 | Example 1

Consider the following VO-fractional reaction–diffusion problem:[33]

$$D_{0,t}^{\nu(t)}\mathfrak{U}(x,t) = \frac{\partial^2 \mathfrak{U}(x,t)}{\partial x^2} + \mathfrak{U}(x,t)\left(1 - \frac{\mathfrak{U}^2(x,t)}{3}\right) + f(x,t), \quad (x,t) \in (0,1)^2, \quad 0 < \nu(t) \leq 1,$$

with initial and boundary conditions

$$\begin{aligned} &\mathfrak{U}(x,0) = 0, \quad x \in [0,1], \\ &\mathfrak{U}(0,t) = 0, \quad \mathfrak{U}(1,t) = t^{3+\nu(t)}, \quad t \in [0,1]. \end{aligned}$$

Here, $f(x,t)$ is such that the exact solution of this problem is $\mathfrak{U}(x,t) = x^2(3-2x)t^{3+\nu(t)}$. The numerical results of the considered problem are reported in Tables 1 and 2 and Figure 2. We have compared the obtained absolute error and maximum absolute error L_∞ for different choices of $\nu(t)$ in Tables 1 and 2, respectively. The achieved outcomes demonstrate that the presented method provides the approximate solutions with high accuracy. In addition, the graphs of approximate solution (left side) and the absolute error (right side) for $\mathcal{K} = 2$ with $\nu(t) = 1$ and $\mathcal{M}_1 = 3, \mathcal{M}_2 = 4$ are shown in Figure 2.

6.2 | Example 2

Consider the following VO-fractional reaction–diffusion problem:[33,34,44]

$$D_{0,t}^{\nu(t)}\mathfrak{U}(x,t) = \frac{\partial^2 \mathfrak{U}(x,t)}{\partial x^2} + f(x,t), \quad (x,t) \in (0,1) \times (0,1], \quad 0 < \nu(t) \leq 1,$$

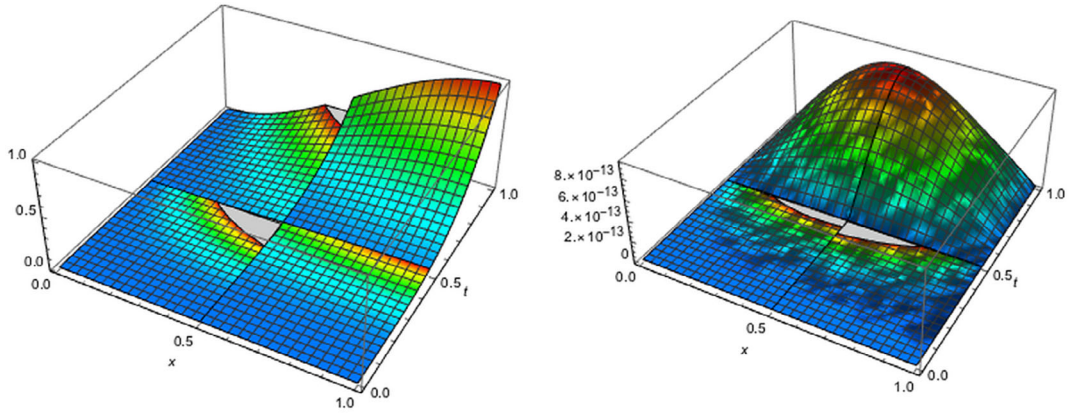

FIGURE 2 The approximate solution (left) and the absolute error (right) for $\mathcal{K} = 2$ with $\nu(t) = 1$ and $\mathcal{M}_1 = 3, \mathcal{M}_2 = 4$ of Example 1

TABLE 3 L_∞-error obtained by the present method and other methods[33,34,44] with $\beta = 2$ of Example 2

$\nu(t)$	$\mathcal{K}$	$\mathcal{M}_1$	$\mathcal{M}_2$	**Present method**
$\frac{\exp(-t)}{300}$	1	2	2	2.4147×10^{-5}
		4	2	5.1466×10^{-8}
		6	2	4.1516×10^{-11}
	2	2	2	2.1877×10^{-6}
		4	2	1.6158×10^{-9}
$\nu(t)$	N	Method in Reference 33	Method in Reference 34	Method in Reference 44
$\frac{\exp(-t)}{300}$	4	9.90×10^{-6}	6.01×10^{-3}	7.13×10^{-3}
	8	1.91×10^{-6}	1.52×10^{-3}	1.12×10^{-3}
	16	8.08×10^{-7}	3.77×10^{-4}	4.67×10^{-4}
	32	1.01×10^{-7}	9.39×10^{-5}	9.56×10^{-5}

with initial and boundary conditions

$$\begin{aligned} &\mathfrak{U}(x,0) = 0, \qquad x \in [0,1], \\ &\mathfrak{U}(0,t) = t^\beta, \qquad \mathfrak{U}(1,t) = \exp(1)t^\beta, \qquad t \in [0,1], \end{aligned}$$

where

$$f(x,t) = \exp(x)t^\beta \left[\frac{\Gamma(\beta+1)}{\Gamma(\beta+1-\nu(t))} t^{-\nu(t)} - 1 \right], \qquad \beta \in \mathbf{R}^+.$$

The exact solution of this problem is $\mathfrak{U}(x,t) = \exp(x)t^\beta$. Table 3 shows the maximum absolute error L_∞ obtained by our method and other methods.[33,34,44] The outcomes display that, by using only a small number of base functions, our method are superior to the methods in References 33,34,44. Moreover, absolute error for various values of $\mathcal{K}, \beta$ are plotted in Figures 3 and 4.

6.3 | Example 3

Consider the following VO-fractional subdiffusion equation:[34]

$$\frac{\partial \mathfrak{U}(x,t)}{\partial t} = D_{0,t}^{1-\nu(x,t)} \left[\frac{\partial^2 \mathfrak{U}(x,t)}{\partial x^2} \right] + f(x,t), \qquad 0 < \nu(x,t) \le 1,$$

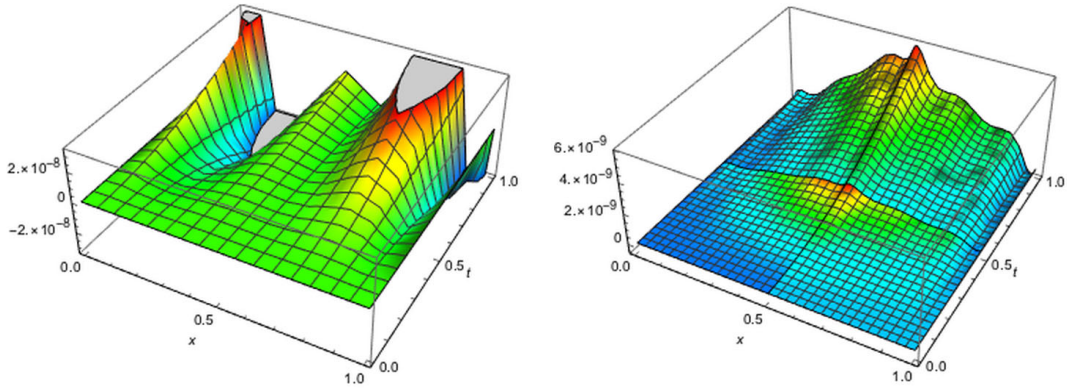

FIGURE 3 Absolute error for $\mathcal{K} = 1$ (left) and $\mathcal{K} = 2$ (right) with $\nu(t) = \frac{2+\sin(t)}{400}$ and $\mathcal{M}_1 = 4, \mathcal{M}_2 = 2, \beta = 2$ of Example 2

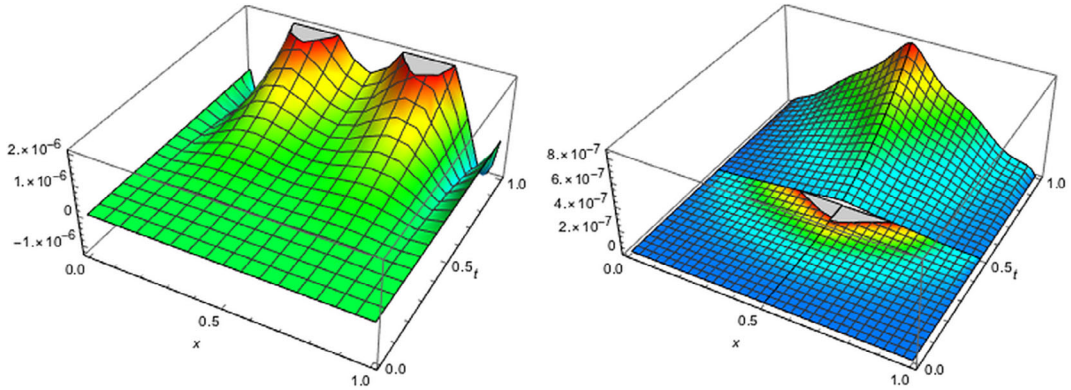

FIGURE 4 Absolute error for $\mathcal{K} = 1$ (left) and $\mathcal{K} = 2$ (right) with $\nu(t) = \frac{2+\sin(t)}{400}$, $\beta = 3$ and $\mathcal{M}_1 = 3, \mathcal{M}_2 = 3$ of Example 2

with initial and boundary conditions

$$\begin{aligned} &\mathfrak{U}(x,0) = 0, \qquad x \in [0,1], \\ &\mathfrak{U}(0,t) = t^2, \qquad \mathfrak{U}(1,t) = \exp(1)t^2, \qquad t \in [0,1], \end{aligned}$$

where

$$f(x,t) = 2\exp(x)\left[t - \frac{t^{1+\nu(x,t)}}{\Gamma(2+\nu(x,t))}\right].$$

The exact solution to this problem is $\mathfrak{U}(x,t) = \exp(x)t^2$. The obtained maximum absolute error and root-mean-square error by means of the proposed method are shown in Table 4. In addition, to validate our numerical solution, we compare the results in Table 4 with the method in Reference 34 for different choices of $\nu(x,t)$. The absolute error at different points is listed in Table 5 to show the approximate solution convergence to the exact solution by increasing the numbers of the basis functions. The $\mathrm{Log}_{10}L_\infty$-error of $\mathfrak{U}(x,t)$ for different choices of $\mathcal{M}_1$ and $\nu(x,t)$ are depicted in Figure 5. From this figure, we can observe that as the number of the basis functions increase, the approximate solutions tend to zero.

6.4 | Example 4

Consider the following VO-fractional reaction–subdiffusion equation:[23,34,45]

$$\frac{\partial \mathfrak{U}(x,t)}{\partial t} = \mathcal{D}_{0,t}^{1-\nu(x,t)}\left[\frac{\partial^2 \mathfrak{U}(x,t)}{\partial x^2}\right] + f(x,t), \qquad 0 < \nu(x,t) \le 1,$$

TABLE 4 Errors for various choices of $\nu(x,t)$, $\mathcal{M}_1, \mathcal{M}_2$ with $\mathcal{K}=1$ of Example 3

Present method	$\nu(x,t)$	$\mathcal{M}_1$	$\mathcal{M}_2$	L_2-error	L_∞-error
	$\frac{\exp(-xt)}{300}$	2	2	3.6845×10^{-5}	2.4175×10^{-5}
		4	2	5.6442×10^{-8}	5.1466×10^{-8}
		8	2	3.6362×10^{-14}	3.3041×10^{-14}
	$\frac{2+\sin(xt)}{400}$	2	2	1.3021×10^{-4}	7.6277×10^{-5}
		4	2	5.5460×10^{-8}	5.0691×10^{-8}
		8	2	3.6048×10^{-14}	3.2928×10^{-14}
Method in Reference 34	$\nu(x,t)$	h	τ	L_2-error	L_∞-error
	$\frac{2+\sin(xt)}{400}$	$\frac{1}{100}$	$\frac{1}{4}$	4.4023×10^{-2}	6.0281×10^{-3}
			$\frac{1}{8}$	1.1081×10^{-2}	1.5171×10^{-3}
			$\frac{1}{16}$	2.7572×10^{-3}	3.7741×10^{-4}
			$\frac{1}{32}$	6.8721×10^{-4}	9.4057×10^{-5}
	$\frac{\exp(-xt)}{300}$	$\frac{1}{100}$	$\frac{1}{4}$	4.4044×10^{-2}	6.0309×10^{-3}
			$\frac{1}{8}$	1.1078×10^{-2}	1.5166×10^{-3}
			$\frac{1}{16}$	2.7545×10^{-3}	3.7704×10^{-4}
			$\frac{1}{32}$	6.8622×10^{-4}	9.3918×10^{-5}

TABLE 5 The obtained absolute error of the proposed method for two choices of $\nu(x,t)$ and $\mathcal{M}_2=2$ with $\mathcal{K}=2$ of Example 3

	$\nu(x,t)=0.5$		$\nu(x,t)=\frac{\exp(-xt)}{300}$	
$x=t$	$\mathcal{M}_1=1$	$\mathcal{M}_1=3$	$\mathcal{M}_1=1$	$\mathcal{M}_1=3$
0.1	3.6970×10^{-7}	5.5146×10^{-10}	7.7528×10^{-7}	1.3409×10^{-9}
0.2	2.2868×10^{-6}	8.6402×10^{-9}	4.1760×10^{-6}	1.2250×10^{-8}
0.3	1.4308×10^{-5}	3.4703×10^{-8}	1.8511×10^{-5}	4.2698×10^{-8}
0.4	5.5099×10^{-5}	9.0441×10^{-8}	6.1459×10^{-5}	1.0256×10^{-7}
0.5	1.1976×10^{-4}	1.9934×10^{-7}	1.2681×10^{-4}	2.1285×10^{-7}
0.6	1.2353×10^{-4}	2.0756×10^{-7}	1.3212×10^{-4}	2.2412×10^{-7}
0.7	6.2693×10^{-5}	2.0884×10^{-7}	7.1316×10^{-5}	2.2556×10^{-7}
0.8	2.2695×10^{-5}	1.7244×10^{-7}	2.9728×10^{-5}	1.8623×10^{-7}
0.9	5.4001×10^{-5}	8.4446×10^{-8}	5.8009×10^{-5}	9.2451×10^{-8}
1	2.9952×10^{-16}	2.9952×10^{-16}	2.9952×10^{-16}	2.9952×10^{-16}

with initial and boundary conditions

$$\begin{aligned} &\mathfrak{U}(x,0)=0, \quad && x\in[0,1],\\ &\mathfrak{U}(0,t)=0, \quad \mathfrak{U}(1,t)=0, && t\in[0,1], \end{aligned}$$

where

$$f(x,t)=\sin(2\pi x)\left[2t+\frac{8\pi^2 t^{1+\nu(x,t)}}{\Gamma(2+\nu(x,t))}\right].$$

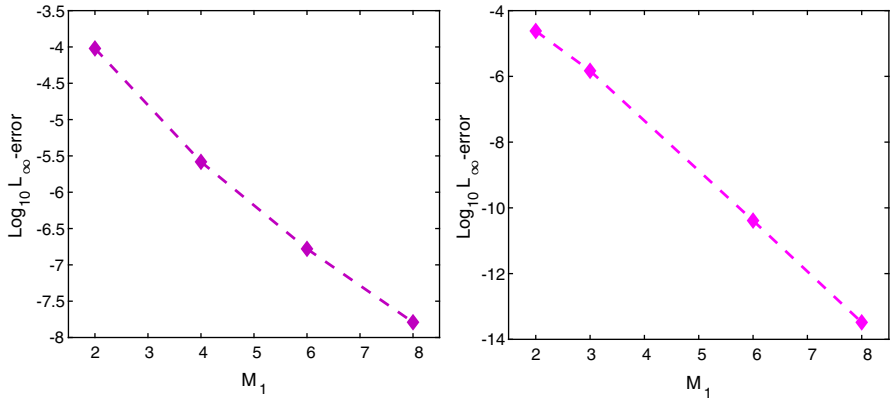

FIGURE 5 $\text{Log}_{10}L_\infty$-error of $\mathfrak{U}(x,t)$ for different choices of $\mathcal{M}_1$ with $\nu(x,t)=\frac{2xt+1}{300}$ (left) and $\nu(x,t)=0.65$ (right) and $\mathcal{M}_2=2, \mathcal{K}=1$ of Example 3

TABLE 6 Absolute errors for various choices of $\nu(x,t)$, $\mathcal{M}_1$ with $\mathcal{M}_2=2$, and $\mathcal{K}=1$ of Example 4

	Present method				Legendre wavelet method[23]	
$x=t$	$\mathcal{M}_1=5$		$\mathcal{M}_1=7$		$\hat{m}=30$ $(k=1, M=15)$	
	$\nu(x,t)=0.25$	$\nu(x,t)=0.5$	$\nu(x,t)=0.25$	$\nu(x,t)=0.5$	$\nu(x,t)=0.25$	$\nu(x,t)=0.5$
0.1	2.3769×10^{-6}	2.3753×10^{-6}	4.7538×10^{-8}	4.8404×10^{-8}	9.8263×10^{-5}	1.2476×10^{-4}
0.2	2.9286×10^{-5}	2.8969×10^{-5}	4.1227×10^{-7}	4.0741×10^{-7}	2.7478×10^{-4}	3.0910×10^{-4}
0.3	2.2096×10^{-5}	2.1548×10^{-5}	2.6596×10^{-7}	2.5796×10^{-7}	4.5835×10^{-4}	4.8715×10^{-4}
0.4	9.9333×10^{-6}	9.5114×10^{-6}	4.7908×10^{-7}	4.7238×10^{-7}	4.4041×10^{-4}	4.5564×10^{-4}
0.5	8.9857×10^{-13}	1.3971×10^{-13}	1.4509×10^{-13}	8.2619×10^{-13}	7.0947×10^{-5}	7.2237×10^{-5}
0.6	2.2550×10^{-5}	2.1928×10^{-5}	1.0811×10^{-6}	1.0712×10^{-6}	8.8728×10^{-4}	8.9738×10^{-4}
0.7	1.2136×10^{-4}	1.2013×10^{-4}	1.4635×10^{-6}	1.4455×10^{-6}	1.9053×10^{-3}	1.9186×10^{-3}
0.8	4.7091×10^{-4}	4.6972×10^{-4}	6.6319×10^{-6}	6.6136×10^{-6}	2.4474×10^{-3}	2.4580×10^{-3}
0.9	1.9249×10^{-4}	1.9251×10^{-4}	3.8158×10^{-6}	3.8223×10^{-6}	1.8924×10^{-3}	1.8976×10^{-3}

TABLE 7 Errors for various choices of $\nu(x,t)$, $\mathcal{M}_1$, $\mathcal{M}_2$, and $\mathcal{K}$ of Example 4

$\nu(x,t)$	$\mathcal{K}$	$\mathcal{M}_1$	$\mathcal{M}_2$	L_2-error	L_∞-error
0.5	1	3	2	1.7130×10^{-2}	1.2261×10^{-2}
	2	3	2	1.4726×10^{-3}	1.0971×10^{-3}
	1	5	2	5.2346×10^{-4}	4.6972×10^{-4}
	1	7	2	7.8769×10^{-6}	6.6136×10^{-6}
$\frac{20-(xt)^2}{500}$	1	3	2	1.7193×10^{-2}	1.2273×10^{-2}
	2	3	2	1.4844×10^{-3}	1.1026×10^{-3}
	1	5	2	5.2589×10^{-4}	4.7177×10^{-4}
	1	7	2	7.9070×10^{-6}	6.6449×10^{-6}

The exact solution of this problem is $\mathfrak{U}(x,t)=\sin(2\pi x)t^2$. To solve this problem, we employ different variable orders of the fractional derivative to clarify the superiority of the proposed method. The behavior of absolute error obtained by the present approach in comparison to the Legendre wavelet method[23] is mentioned in Table 6. Moreover, the maximum absolute errors and root-mean-square errors are demonstrated in Table 7. The proposed problem has also been discussed by compact finite difference method (Table 6)[45] for $\nu(x,t)=0.5, \tau=\frac{1}{4000}$ and $h=\frac{1}{16}$. So that, in Reference 45 the maximum absolute error has been obtained 9.6041×10^{-5}. From our results and Table 6 in Reference 45 it can be seen that the proposed method has a higher accuracy.

TABLE 8 Errors for various choices of $\mathcal{M}_1, \mathcal{K}$ with $\nu(x,t) = \frac{15+\cos(xt)}{300}$ and $\mathcal{M}_2 = 2$ of Example 5

$\mathcal{K}$	$\mathcal{M}_1$	L_2-error	L_∞-error
1	2	3.6802×10^{-5}	2.4145×10^{-5}
	4	5.6413×10^{-8}	5.1465×10^{-8}
	6	4.8395×10^{-11}	4.1529×10^{-11}
	8	3.8363×10^{-14}	3.3058×10^{-14}
2	2	3.1608×10^{-6}	2.1592×10^{-6}
	4	3.1923×10^{-9}	1.5591×10^{-9}

FIGURE 6 $\text{Log}_{10} L_\infty$-error of $\mathfrak{U}(x,t)$ for different choices of $\mathcal{M}_1$ with $\nu(x,t) = \frac{\exp(xt)+\sin(xt)}{50}$ and $\mathcal{M}_2 = 2, \mathcal{K} = 1$ of Example 5

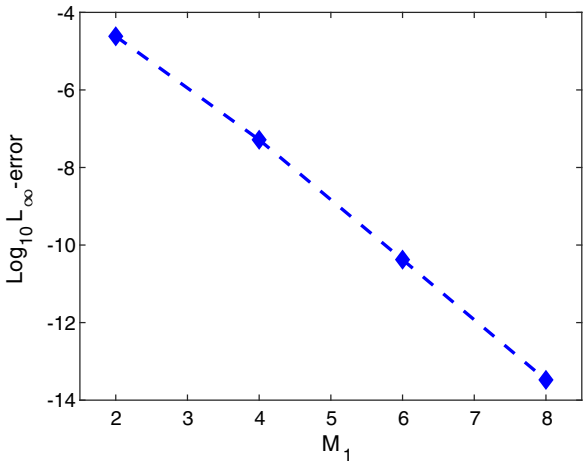

6.5 | Example 5

Consider the following VO-fractional reaction–subdiffusion equation:[46]

$$\frac{\partial \mathfrak{U}(x,t)}{\partial t} = D_{0,t}^{1-\nu(x,t)} \left[\frac{\partial^2 \mathfrak{U}(x,t)}{\partial x^2} - \mathfrak{U}(x,t) \right] + \mathfrak{U}^2(x,t) + f(x,t), \qquad 0 < \nu(x,t) \leq 1,$$

with initial and boundary conditions

$$\mathfrak{U}(x,0) = 0, \qquad x \in [0,1],$$
$$\mathfrak{U}(0,t) = t^2, \qquad \mathfrak{U}(1,t) = \exp(1)t^2, \qquad t \in [0,1],$$

where

$$f(x,t) = \exp(x)t[2 - \exp(x)t^3].$$

The exact solution to this problem is $\mathfrak{U}(x,t) = \exp(x)t^2$. The maximum of the absolute errors and root-mean-square errors for various choices of $\mathcal{M}_1, \mathcal{K}$ with $\nu(x,t) = \frac{15+\cos(xt)}{300}$ and $\mathcal{M}_2 = 2$ are demonstrated in Table 8. From the outcomes, it can be found that by increasing the number of basis functions, the approximate solution converges to the exact solution. Furthermore, to illustrate the effect of the proposed method in resolving the problem, we illustrate the numerical results in Figures 6 and 7. The proposed problem has also been discussed in Reference 46 and the results are given in Tables 1 and 2. From our results in Figures 6 and 7 and Tables 1 and 2 in Reference 46 it is seen that the proposed method has a higher accuracy.

7 | CONCLUSION

In this article, we first introduced the novel LMWFs and their attributes. Then, we presented the technique for calculating the modified and pseudo-operational matrices. These matrices with special characteristics affect the numerical

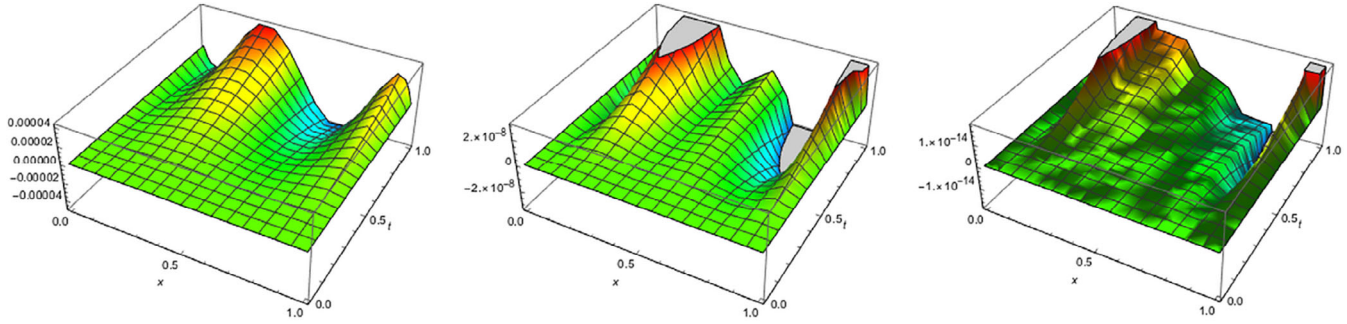

FIGURE 7 Absolute error of $\mathfrak{U}(x,t)$ for $\mathcal{M}_1 = 2$ (left) $\mathcal{M}_1 = 4$ (center) $\mathcal{M}_1 = 8$ (right) with $v(x,t) = \frac{15-x^2+t^4}{400}$ and $\mathcal{M}_2 = 2, \mathcal{K} = 1$ of Example 5

method and make the approximate solution with high precision. A discrete scheme using LMWFs for VO fractional reaction-diffusion and subdiffusion equations are proposed. Finally, we compare the results with exact solutions and some other methods in graphs and tables to demonstrate the efficiency and applicability of the proposed scheme. Some of the advantages of the present technique are summarized as:

- Few terms of LMWFs are required to achieve effective and accurate results.
- The accuracy of the MOM directly affects the method process.
- The operational matrices have a lot of zero components that cause little CPU time.
- Implementing this method is very convenient and effective for other kinds of fractional partial differential equations.

ACKNOWLEDGMENTS

This work is supported by the National Elite Foundation and Alzahra University. We express our sincere thanks to the anonymous referees for their valuable suggestions that improved the final article.

CONFLICT OF INTEREST

This work does not have any conflicts of interest.

AUTHOR CONTRIBUTIONS

Haniye Dehestani and Yadollah Ordokhani conceived of the presented idea. Haniye Dehestani developed the theory and performed the computations. Yadollah Ordokhani and Mohsen Razzaghi verified the analytical methods. Yadollah Ordokhani encouraged Haniye Dehestani to investigate a new method and supervised the findings of this work. Haniye Dehestani, Yadollah Ordokhani and Mohsen Razzaghi contributed to the design and implementation of the research, to the analysis of the results and to the writing of the article.

ORCID

Yadollah Ordokhani https://orcid.org/0000-0002-5167-6874

REFERENCES

1. Coimbra CF. Mechanics with variable-order differential operators. Ann Phys. 2003;12(11-12):692–703.
2. Lorenzo C, Hartley T. Initialization, conceptualization, and application in the generalized fractional calculus. Cleveland, OH; National Aeronautics and Space Administration, Lewis Research Center, 1998 NASA/Tp-1998-208415.
3. Diaz G, Coimbra C. Nonlinear dynamics and control of a variable order oscillator with application to the van der Pol equation. Nonlinear Dyn. 2009;56(1-2):145–157.
4. Ramirez LE, Coimbra CF. A variable order constitutive relation for viscoelasticity. Ann Phys. 2007;16(7-8):543–552.
5. Orosco J, Coimbra C. On the control and stability of variable-order mechanical systems. Nonlinear Dyn. 2016;86(1):695–710.
6. Ostalczyk P, Rybicki T. Variable-fractional-order dead-beat control of an electromagnetic servo. J Vib Control. 2008;14(9-10):1457–1471.
7. Ingman D, Suzdalnitsky J. Control of damping oscillations by fractional differential operator with time-dependent order. Comput Methods Appl Mech Eng. 2004;193(52):5585–5595.

8. Moghaddam BP, JAT M. A stable three-level explicit spline finite difference scheme for a class of nonlinear time variable order fractional partial differential equations. Comput Math Appl. 2017;73(6):1262–1269.
9. Zahra W, Hikal M. Non standard finite difference method for solving variable order fractional optimal control problems. J Vib Control. 2017;23(6):948–958.
10. Dehestani H, Ordokhani Y, Razzaghi M. Application of the modified operational matrices in multiterm variable-order time-fractional partial differential equations. Math Meth Appl Sci. 2019;42(18):7296–7313.
11. Dehestani H, Ordokhani Y, Razzaghi M. Pseudo-operational matrix method for the solution of variable-order fractional partial integro-differential equations. Eng Comput. 2020;1–16.
12. Doha E, Abdelkawy M, Amin A, Baleanu D. Spectral technique for solving variable-order fractional Volterra integro-differential equations. Numer Methods Partial Differ Equ. 2018;34(5):1659–1677.
13. Balakrishnan V. Anomalous diffusion in one dimension. Physica A. 1985;132(2-3):569–580.
14. Giona M, Roman HE. Fractional diffusion equation for transport phenomena in random media. Physica A. 1992;185(1-4):87–97.
15. Gorenflo R, Mainardi F, Moretti D, Pagnini G, Paradisi P. Discrete random walk models for space–time fractional diffusion. Chem Phys. 2002;284(1-2):521–541.
16. Henry BI, Wearne SL. Fractional reaction–diffusion. Physica A. 2000;276(3-4):448–455.
17. Kosztołowicz T. Subdiffusion in a system with a thick membrane. J Membr Sci. 2008;320(1-2):492–499.
18. Abad E, Yuste S, Lindenberg K. Reaction-subdiffusion and reaction-superdiffusion equations for evanescent particles performing continuous-time random walks. Phys Rev E. 2010;81(3):031115.
19. Langlands T, Henry BI, Wearne SL. Anomalous subdiffusion with multispecies linear reaction dynamics. Phys Rev E. 2008;77(2):021111.
20. Adel M. Finite difference approach for variable order reaction–subdiffusion equations. Adv Differ Equ. 2018;2018(1):1–12.
21. Sweilam N, Ahmed S, Adel M. A simple numerical method for two-dimensional nonlinear fractional anomalous sub-diffusion equations. Math Methods Appl Sci. 2020.
22. Yan ZZ, Zheng CF, Zhang C. The Monte Carlo Markov chain method for solving the modified anomalous fractional sub-diffusion equation. J Comput Phys. 2019;394:477–490.
23. Heydari M. Wavelets Galerkin method for the fractional subdiffusion equation. J Comput Nonlinear Dyn. 2016;11(6).
24. Yaseen M, Abbas M, Ismail AI, Nazir T. A cubic trigonometric B-spline collocation approach for the fractional sub-diffusion equations. Appl Math Comput. 2017;293:311–319.
25. Dehestani H, Ordokhani Y, Razzaghi M. Fractional-Lucas optimization method for evaluating the approximate solution of the multi-dimensional fractional differential equations. Eng Comput. 2021. https://doi.org/10.1007/s00366-020-01048-1.
26. Oruç Ö. A new algorithm based on Lucas polynomials for approximate solution of 1D and 2D nonlinear generalized Benjamin–Bona–Mahony–Burgers equation. Comput Math Appl. 2017;74(12):3042–3057.
27. Oruç Ö. A new numerical treatment based on Lucas polynomials for 1D and 2D sinh-Gordon equation. Commun Nonlinear Sci Numer Simul. 2018;57:14–25.
28. Dehestani H, Ordokhani Y, Razzaghi M. On the applicability of Genocchi wavelet method for different kinds of fractional-order differential equations with delay. Numer Linear Algebra Appl. 2019;26(5):e2259.
29. Sahu PK, Ray SS. Legendre wavelets operational method for the numerical solutions of nonlinear Volterra integro-differential equations system. Appl Math Comput. 2015;256:715–723.
30. Heydari MH, Avazzadeh Z, Haromi MF. A wavelet approach for solving multi-term variable-order time fractional diffusion-wave equation. Appl Math Comput. 2019;341:215–228.
31. Khader M, Adel M. Chebyshev wavelet procedure for solving FLDEs. Acta Appl Math. 2018;158(1):1–10.
32. Zhang J, Zhang X, Yang B. An approximation scheme for the time fractional convection–diffusion equation. Appl Math Comput. 2018;335:305–312.
33. Hajipour M, Jajarmi A, Baleanu D, Sun H. On an accurate discretization of a variable-order fractional reaction-diffusion equation. Commun Nonlinear Sci Numer Simul. 2019;69:119–133.
34. Cao J, Qiu Y, Song G. A compact finite difference scheme for variable order subdiffusion equation. Commun Nonlinear Sci Numer Simul. 2017;48:140–149.
35. Yu H, Wu B, Zhang D. A generalized Laguerre spectral Petrov–Galerkin method for the time-fractional subdiffusion equation on the semi-infinite domain. Appl Math Comput. 2018;331:96–111.
36. Ghaffari R, Ghoreishi F. Reduced spline method based on a proper orthogonal decomposition technique for fractional sub-diffusion equations. Appl Numer Math. 2019;137:62–79.
37. Dehghan M, Abbaszadeh M, Mohebbi A. Error estimate for the numerical solution of fractional reaction–subdiffusion process based on a meshless method. J Comput Appl Math. 2015;280:14–36.
38. Li C, Zhao Z, Chen Y. Numerical approximation of nonlinear fractional differential equations with subdiffusion and superdiffusion. Comput Math Appl. 2011;62(3):855–875.
39. Heydari M, Mahmoudi M, Shakiba A, Avazzadeh Z. Chebyshev cardinal wavelets and their application in solving nonlinear stochastic differential equations with fractional Brownian motion. Commun Nonlinear Sci Numer Simul. 2018;64:98–121.
40. Dehestani H, Ordokhani Y, Razzaghi M. Combination of Lucas wavelets with Legendre-Gauss quadrature for fractional Fredholm-Volterra integro-differential equations. J Comput Appl Math. 2021;382:113070.
41. Dehestani H, Ordokhani Y, Razzaghi M. Fractional-order Legendre–Laguerre functions and their applications in fractional partial differential equations. Appl Math Comput. 2018;336:433–453.

42. Koshy T. Fibonacci and lucas numbers with applications. New York, NY: Wiley, 2001.
43. Byrd PF. Expansion of analytic functions in polynomials associated with fibonacci numbers. Fibonacci Quart. 1963;1:16.
44. Chen CM, Liu F, Anh V, Turner I. Numerical schemes with high spatial accuracy for a variable-order anomalous subdiffusion equation. SIAM J Sci Comput. 2010;32(4):1740–1760.
45. Wang Z, Vong S. Compact difference schemes for the modified anomalous fractional sub-diffusion equation and the fractional diffusion-wave equation. J Comput Phys. 2014;277:1–15.
46. Chen CM, Liu F, Turner I, Anh V, Chen Y. Numerical approximation for a variable-order nonlinear reaction–subdiffusion equation. Numer Algorithms. 2013;63(2):265–290.

How to cite this article: Dehestani H, Ordokhani Y, Razzaghi M. A novel direct method based on the Lucas multiwavelet functions for variable-order fractional reaction-diffusion and subdiffusion equations. *Numer Linear Algebra Appl*. 2021;28:e2346. https://doi.org/10.1002/nla.2346